

# Inhibition of erythropoiesis in malaria anemia: role of hemozoin and hemozoin-generated 4-hydroxynonenal

\*Oleksii A. Skorokhod,<sup>1</sup> \*Luisa Caione,<sup>2</sup> Tiziana Marrocco,<sup>1</sup> Giorgia Migliardi,<sup>2</sup> Valentina Barrera,<sup>1</sup> Paolo Arese,<sup>1</sup> Wanda Piacibello,<sup>2</sup> and Evelin Schwarzer<sup>1</sup>

<sup>1</sup>Department of Genetics, Biology, and Biochemistry, and <sup>2</sup>Institute for Cancer Research and Treatment, Laboratory of Cell Therapy, University of Torino Medical School, Torino, Italy

**Severe malaria anemia is characterized by inhibited/alterred erythropoiesis and presence of hemozoin-(HZ)-laden bone-marrow macrophages. HZ mediates peroxidation of unsaturated fatty acids and production of bioactive aldehydes such as 4-hydroxynonenal (HNE). HZ-laden human monocytes inhibited growth of cocultivated human erythroid cells and produced HNE that diffused to adjacent cells generating HNE-protein adducts. Cocultivation with HZ or treatment with low micromolar HNE inhibited growth of ery-**

**throid cells interfering with cell cycle without apoptosis. After HZ/HNE treatment, 2 critical proteins in cell-cycle regulation, p53 and p21, were increased and the retinoblastoma protein, central regulator of G<sub>1</sub>-to-S-phase transition, was consequently hypophosphorylated, while GATA-1, master transcription factor in erythropoiesis was reduced. The resultant decreased expression of cyclin A and D2 retarded cell-cycle progression in erythroid cells and the K562 cell line. As a second major effect, HZ and HNE inhibited**

**protein expression of crucial receptors (R): transferrinR1, stem cell factorR, interleukin-3R, and erythropoietinR. The reduced receptor expression and the impaired cell-cycle activity decreased the production of cells expressing glycophorin-A and hemoglobin. Present data confirm the inhibitory role of HZ, identify HNE as one HZ-generated inhibitory molecule and describe molecular targets of HNE in erythroid progenitors possibly involved in erythropoiesis inhibition in malaria anemia. (Blood. 2010;116(20):4328-4337)**

## Introduction

Severe malaria anemia (SMA) is a frequent complication and an important cause of mortality in children and pregnant women.<sup>1</sup> SMA is due to enhanced removal of parasitized and nonparasitized erythrocytes (red blood cells [RBCs]) and inhibited erythropoiesis.

The latter is characterized by low reticulocyte response,<sup>2</sup> normal or increased production of erythropoietin (EPO),<sup>3</sup> and altered morphology of erythroid precursors.<sup>4-8</sup> Erythroid growth and differentiation occurs in the erythroblastic island, where erythroid precursors proliferate, differentiate, and enucleate to reticulocytes in close contact to a central macrophage that provides adjacent precursors with iron and supportive (or inhibitory) cytokines, chemokines, and growth factors.<sup>9</sup> Postmortem analysis of bone marrow (BM) sections has shown massive presence of malaria pigment hemozoin (HZ) in BM macrophages,<sup>5,7,8</sup> which intensely phagocytose HZ as residual bodies or HZ-containing mature parasite stages. In severe malaria, a remarkable association was shown to exist between the prevalence of HZ-laden BM macrophages and morphologic abnormalities of erythroid cell,<sup>4-7</sup> reticulocyte suppression,<sup>1,2,8</sup> and severity of anemia.<sup>6-8</sup> Interestingly, reports have shown changes in the cell-cycle distribution in erythroblasts and an ineffective erythropoiesis in BM aspirates of Gambian children<sup>10</sup> and non- and semi-immune adults<sup>4</sup> suffering from malaria anemia.

Native HZ, largely coincident with the residual body expelled after schizogony, contains a scaffold of crystalline cyclic heme dimers ( $\beta$ -hematin) and large amounts of polyunsaturated fatty acids that are nonenzymatically peroxidized and broken down by

HZ-iron to terminal hydroxyaldehydes such as 4-hydroxynonenal (HNE).<sup>11-13</sup> HNE is a highly bioactive, predominantly lipophilic molecule that binds to amino-, histidyl-, and thiol groups of proteins and to DNA forming covalent, stable HNE-adducts.<sup>14</sup> HNE, present in high concentrations in HZ and HZ-laden human monocytes,<sup>12,13</sup> was shown to shed from HZ or HZ-fed monocytes and inhibit dose-dependently the ex vivo growth of erythroid progenitors by an undisclosed mechanism.<sup>15</sup>

Aims of this study were to confirm the inhibitory role of HZ on erythropoiesis, to identify the responsible molecule(s) and to understand its (their) mechanism of action. To this end, we analyzed, first, the production of HNE by HZ or HZ-laden human monocytes and its transfer to cocultivated primary erythroid cells differentiating from CD34<sup>+</sup> cells to hemoglobin-producing precursors and finally mature RBCs; second, the effect of HZ and HNE on cell cycle and expression of crucial receptors, by analogy with observations on cell lines<sup>16</sup>; and third, the effects of HZ and HNE on the transcription factor p53, the cyclin kinase inhibitor p21, the retinoblastoma protein, and cyclins, main regulators of the cell cycle,<sup>17,18</sup> and GATA-1, crucial controller of both cell-cycle and receptor expression.<sup>19</sup> We show that HZ-laden monocytes, native HZ, and low-micromolar HNE-induced growth inhibition of cocultivated human erythroid cells interfering with cell cycle and down-modulating the receptors for transferrin R1 (TFR1), stem cell factor (SCFR, c-kit, CD71), interleukin-3 (IL-3R), and erythropoietin (EPOR) without inducing apoptosis. The impaired cell cycle

Submitted March 10, 2010; accepted July 23, 2010. Prepublished online as *Blood* First Edition paper, August 4, 2010; DOI 10.1182/blood-2010-03-272781.

\*O.A.S. and L.C. contributed equally to this article.

The online version of this article contains a data supplement.

The publication costs of this article were defrayed in part by page charge payment. Therefore, and solely to indicate this fact, this article is hereby marked "advertisement" in accordance with 18 USC section 1734.

© 2010 by The American Society of Hematology

and reduced receptor expression decreased the total cell yield and the yield of differentiated erythroid cells.

In conclusion, present data confirm the inhibitory role of HZ, identify HNE as one inhibitory molecule, and describe multiple molecular targets of HNE in erythroid precursors possibly involved in the mechanism of erythropoiesis inhibition in malaria.

## Methods

### Reagents

Unless otherwise stated, reagents were from Sigma-Aldrich.

### Isolation of CD34<sup>+</sup> cells and erythroid cell growth in liquid culture

Umbilical cord blood was obtained at the end of full-term pregnancies with written informed consent in accordance with the Declaration of Helsinki. Mononuclear cells were isolated from cord blood using Lymphoprep (Sentinel) density gradient centrifugation. CD34<sup>+</sup> cells were isolated using a magnetic immunoseparation device (miniMACS; Miltenyi Biotec). Efficiency was verified by flow cytometry (FACS) counterstaining with a CD34<sup>+</sup>-phycoerythrin antibody (PE; HPCA-2; BD Biosciences). CD34<sup>+</sup>-enriched cells were seeded at  $2.5 \times 10^4$  cells/mL and grown in the erythroid cell basic medium (EBM),<sup>20</sup> supplemented with 5% (vol/vol) fetal calf serum (HyClone) at 37°C and 5% CO<sub>2</sub>. During the first step (days 0-8) of differentiation, EBM was supplemented with recombinant human (rh) erythropoietin (rhEPO, 3 U/mL; Eprex; Cilag), rh stem cell factor (rhSCF, 100 ng/mL; a gift from Amgen), rh human interleukin-3 (rhIL-3, 5 ng/mL; Sandoz-Novartis), and hydrocortisone (10 μM; EBM-S) and changed every fourth day. From day 8, cells were cocultivated for 3 days on adherent cell layer of the murine stroma cell line MS-5 in fresh EBM supplemented with rhEpo (3 U/mL), and from day 11 until day 26, in EBM without supplementations. In some experiments the CD34<sup>+</sup> cells were first expanded in Iscove's modified Dulbecco medium supplemented with 10% (vol/vol) fetal calf serum, Flt3-ligand (50 ng/mL, Amgen), rhSCF (50 ng/mL), rh thrombopoietin (rhTPO, 10 ng/mL; a gift from Kirin Brewery), rh interleukin-6 (rhIL-6, 10 ng/mL; PeproTech) at 37°C and 5% CO<sub>2</sub> for 7 days before differentiation.<sup>21</sup> The use of human cells obtained after written informed consent as described for the present work was approved by the Bioethical Committee of the Torino University School of Medicine, the institutional review board for these studies.

### Erythroid cell growth in semisolid culture: BFU-E and CFU-E studies

Burst forming units-erythroid (BFU-E) and colony forming units-erythroid (CFU-E) were assayed in semisolid methylcellulose cultures as described.<sup>22</sup> One thousand primary CD34<sup>+</sup> progenitors from liquid cultures, treated or not with HZ or HNE, were seeded and CFU-Es, BFU-Es, and colony-forming units granulocyte-macrophage (CFU-GM) colonies were enumerated after 7, 14, and 14 days of incubation, respectively.

### MS-5 cell line

Before cocultivation with erythroid cells, murine stromal cells (line MS-5) were grown in minimum essential media (Gibco) supplemented with 2-mercaptoethanol (50 μM), 12.5% (vol/vol) fetal bovine serum, and 12.5% (vol/vol) horse serum (Gibco).

### K562 cell line

Cells of the immortalized cell line K562 with proliferative and antigenic characteristics similar to erythroid cells were used to confirm results obtained with erythroid cells and to perform cell-cycle studies.<sup>23</sup> K562 cells were cultivated at  $10^5$  cells/mL EBM-S and treated or not with 25 μM HZ (HZ-heme content) or 7 μM HNE like erythroid cultures.

### Isolation, quantification, and opsonization of HZ and control human RBCs

*Plasmodium falciparum* parasites (Palo Alto strain, mycoplasma-free) were kept in culture as described.<sup>15</sup> Culture supernatant was separated after schizogony on a Percoll density gradient, and HZ collected from the 10/40% interphase and treated as described.<sup>24</sup> HZ-heme was quantified by luminescence and added either directly to the erythroid cells or after opsonization with fresh human AB serum for 30 minutes at 37°C to adherent monocytes for phagocytosis.<sup>24</sup> Control human RBCs were opsonized with immunoglobulin G (IgG) anti-D (Partobulin) as indicated.<sup>24</sup>

### Handling of human monocytes and phagocytosis of HZ or RBCs

Monocytes were isolated from peripheral blood of healthy human donors by centrifugation on Ficoll, resuspended in RPMI 1640 supplemented with 2mM L-glutamine, 1mM sodium pyruvate, 1% penicillin/streptomycin, 0.1mM nonessential amino acids (RS), and plated. After 60 minutes incubation at 37°C, nonadherent cells were removed by 3 washings and RS was added. Phagocytosis was started by adding either 25 μM opsonized HZ-heme (corresponding to 12 RBCs/monocyte in terms of heme content) or opsonized RBCs at 50 RBCs/monocyte. After 3 hours incubation, nonphagocytosed HZ was removed by 3 washings, and phagocytosed HZ and RBCs were quantified as indicated.<sup>24</sup>

### Cocultivation of erythroid cells with HZ-fed human monocytes, HZ, and HNE

Primary erythroid cells (25 000 cells/mL) were cocultivated with HZ or adherent HZ/RBC-fed or unfed monocytes, or treated with HNE in EBM-S. HZ- or RBC-fed or unfed monocytes were cocultivated at an erythroid cell to monocyte ratio of 1:1 on day 0, while due to erythroid cell proliferation the ratio reached 10:1 on day 4 of cocultivation. HZ was dispersed by several passes through a 27-G-1.2-cm needle and added to the liquid cultures on day 0 at a final concentration of 25 μM HZ-heme and cocultivated up to day 26. HNE (Biomol) was added to the cells at 7 μM final concentration on day 0 and after each medium change every 4th day.

### Detection of HNE-protein adducts

The HNE-protein adducts on the cell surface and the percentage of HNE adduct highly positive cells were assayed by flow cytometry (FACS, FACSCalibur; BD Biosciences) after labeling with an anti-HNE-adduct antibody (Alexis Biochemicals) and fluorescein isothiocyanate (FITC)-conjugated F(ab)<sub>2</sub> goat anti-rabbit IgG.<sup>13</sup>

### Phenotypic analysis of erythroid cells

Labeling and subsequent phenotypic analysis of erythroid cells harvested at indicated days was performed by FACS direct immunofluorescence. Saturating concentrations of the following surface antigen recognizing monoclonal antibodies were used. Anti-CD34<sup>+</sup>-FITC (MEC 14-7), anti-TfR1 (CD71)-FITC (Ber-T9), anti-glycophorin A-RPE (JC159), anti-SCFR (CD117, c-kit)-FITC (104D2) were from Dako; anti-IL-3R (CD123)-PE-Cy5 (9F5) was from BD Pharmingen; and anti-EPOR (38 409) was from R&D Systems. Bound anti-EPOR antibodies were detected by FITC-conjugated anti-mouse IgG. Receptor recognition by the antibodies was not influenced by 7 μM HNE (not shown). Mean fluorescence intensity (MFI) was measured by FACS and data analyzed with CellQuest (BD Biosciences) or WinMDI (Scripps Research Institute) software. Hemoglobin was quantified by the Drabkin method.

### Proliferation and apoptosis assay

Viable erythroid cells were counted by trypan blue exclusion at indicated days. Apoptosis was measured by 2 FACS-based methods: first, by Annexin V-FITC staining following the manufacturer's specifications (Apoptosis Detection Kit; Sigma-Aldrich); second, by propidium iodide (PI) nucleus labeling to reveal apoptotic nuclei in the subdiploid region of the cell-cycle

histogram. In brief, 0.1-0.2 million washed cells were resuspended in a hypotonic PI solution (50  $\mu$ g/mL PI, 0.1% sodium citrate, 0.4 mg/mL DNase-free RNase, type 1-A, 0.1% [vol/vol] Triton X-100). After 30 minutes incubation on ice in the dark, the fluorescence was acquired by FACS, and the percentage of cells in the subdiploid region (on the left of the diploid peak in the DNA staining distribution) was considered as the share of apoptotic cells.<sup>25</sup>

### Cell-cycle analysis

Cell-cycle analysis was performed as indicated.<sup>26</sup> In brief, washed cells were resuspended in PBS containing 0.1% (wt/vol) sodium citrate, 0.4 mg/mL DNase-free RNase, type 1-A, 0.1% (vol/vol) Triton X-100, and 50  $\mu$ g/mL PI. After 30 minutes at room temperature (RT) in the dark, cellular DNA content was analyzed by FACS measuring the PI binding intensity of the cells. Histograms displayed a double-peak distribution of cellular PI intensity, whereby the left peak represents cells in G<sub>0</sub>/G<sub>1</sub>-phase, the "interpeak" interval cells in S-phase, and the right peak cells in G<sub>2</sub>/M-phase.

### Immunoblotting

Cells were washed in presence of protease inhibitor cocktail Complete (Roche Diagnostics) at 4°C and solubilized in Laemmli buffer after the addition of 5mM N-ethylmaleimide. The proteins (10-30  $\mu$ g) were separated in a 10% (wt/vol) acrylamide sodium dodecyl sulfate polyacrylamide gel electrophoresis (SDS-PAGE) and transferred onto nitrocellulose (Amersham Biosciences). After saturation with 5% (wt/vol) skimmed milk powder dissolved in phosphate-buffered saline-Tween 0.1% (PBS-T), the membrane was exposed to following monoclonals: mouse anti-CD71, clone H68.4 (Zymed, Invitrogen) at 1:1000 dilution; mouse anti-p21, clone 187 at 1:1000 dilution; rabbit polyclonal anti-p53 at 1:500 dilution; mouse anti-cyclin A, clone BF683 at 1:2000 dilution; rabbit polyclonal anti-cyclin D2, anti-cyclin B1 at 1:1000 dilution (all Santa Cruz Biotechnology), and rabbit monoclonal anti-GATA-1, clone D52H6 (Cell Signaling Technology) at 1:1000 dilution. The bound antibodies were detected with anti-mouse or anti-rabbit horseradish peroxidase-conjugated antibodies (Amersham) by enhanced chemiluminescence (ECL).

### Immunostaining and microscopy

Washed K562 cells were incubated in PBS supplemented with 1% (vol/vol) human AB serum for 15 minutes at RT and anti-HNE-adduct rabbit polyclonal antibody (1:25 final dilution; Alexis) was added for 30 minutes at 4°C to label surface HNE-adducts. After 4 washes in serum-supplemented PBS, the secondary anti-rabbit FITC-conjugated antibody was added for 30 minutes at RT in the dark. Mowiol solution, containing 13% (vol/vol) Mowiol40-88, 33% (vol/vol) glycerol, 2% (vol/vol) diazobicyclic(2,2,2)-octane, 130mM Tris-HCl, pH 8.5, was used to mount slides. Images were acquired by 63 $\times$  Leica (Wetzlar) oil planar apochromatic objective with 1.32 numerical aperture in a Leica-TCS SP2 spectral confocal microscope using the Leica-LSC image software. Excitation/emission for green channel was 488/514 nm wavelength from the Ar/Kr laser.

### Statistical analysis

Mann-Whitney test was used to compare means between independent groups and determine significance of differences.

## Results

### Inhibition of erythroid cell growth and formation of HNE adducts in erythroid cells cocultivated with HZ-fed human monocytes or HZ or treated with HNE

HZ-fed human monocytes inhibited growth of cocultivated erythroid cells and produced HNE, which diffuses to adjacent cells

forming HNE adducts with surface proteins. Erythroid cells were cocultivated during 4 days with HZ-fed monocytes at a erythroid cell per monocyte ratio of 1:1 at day 0 and 10:1 at day 4. As shown in Figure 1A, HZ-fed monocytes inhibited growth of erythroid cells by approximately 60% compared with unfed monocytes, while growth was not modified when cells were cocultivated with RBC-fed monocytes. Compared with unfed/RBC-fed monocytes, erythroid cells cocultivated with HZ-fed monocytes displayed 2.1- to 2.7-fold greater, time-dependent increase of HNE adducts with surface proteins (Figure 1B-C), indicating that HNE generated within the HZ-fed monocyte can diffuse to and react with adjacent cells.<sup>13</sup>

In long-term experiments (26 days), cocultivation of erythroid cells with HZ (25 $\mu$ M HZ-heme) or supplementation with 7 $\mu$ M HNE (final concentration, added at each fourth day) inhibited cell growth. As shown in Figure 1D, control erythroid cells grew exponentially in liquid culture until day 15 and reached a plateau at day 18 as described.<sup>20</sup> HZ- and HNE-treated cells grew significantly slower ( $-29\% \pm 4\%$  and  $-32\% \pm 2\%$ ,  $P < .05$ ) as controls and reached a growth plateau at  $69\% \pm 2\%$  and  $71\% \pm 2\%$  of control growth, respectively (Figure 1D).

As shown in Figure 1E and F, after 1 and 2 days of cocultivation with HZ, the level of HNE membrane adducts was 100% and 170% higher than in controls, respectively. The percentage of erythroid cells highly positive for HNE membrane adducts was 1.5-fold higher at day 1 and remained 1.3- to 2-fold higher than in controls during the whole incubation time (see supplemental Figure 1, available on the *Blood* Web site; see the Supplemental Materials link at the top of the online article). The extensive and immediate adduct formation in erythroid cells cocultivated with HZ or supplemented with exogenous HNE was transient (Figure 1E) and possibly due to a transient overburden of the cellular HNE degradation and repair mechanisms,<sup>14</sup> which seem not to operate at the same extent in erythroid cultures cocultivated with HZ-laden monocytes (Figure 1B) where HNE was generated in a progressive way and adducts appeared more slowly.

The HNE-surface adduct formation by HZ and HNE was confirmed in K562 cells (Figure S2A). The fluorescence micrographs (supplemental Figure 2B) of HZ-coincubated cells clearly show the formation of HNE adducts. The cell surface appears uniformly covered with green fluorescent HNE adducts. Note the high adduct concentration close to the HZ clumps adherent to the cells. Control cells were negative for green fluorescence. Morphologic examination of erythroid cultures after 21 days of growth in presence of HZ/HNE showed low numbers of mature RBCs and relatively high numbers of erythroblasts, indicating that HZ/HNE treatment also inhibited erythroid cell differentiation (Figure 2). HZ/HNE treatments did not induce apoptosis in erythroid cells during the whole cocultivation period as evidenced by annexin V/PI-binding and trypan blue exclusion test. The apoptosis rate in erythroid cells cocultivated with HZ-fed monocytes or HZ, or treated with HNE was below 6% and identical with apoptosis rate in control cultures as shown for the first 4 culture days in supplemental Table 1. Apoptosis and cell death can therefore be excluded as the cause of reduced cell growth due to treatments.

### Inhibition of BFU-E and CFU-E in erythroid cells cocultivated with HZ or treated with HNE

Aliquots of the liquid erythroid cell culture were taken at different time points and checked for their ability to develop into colonies in the presence of suitable growth factors such as SCF, EPO, and IL-3.

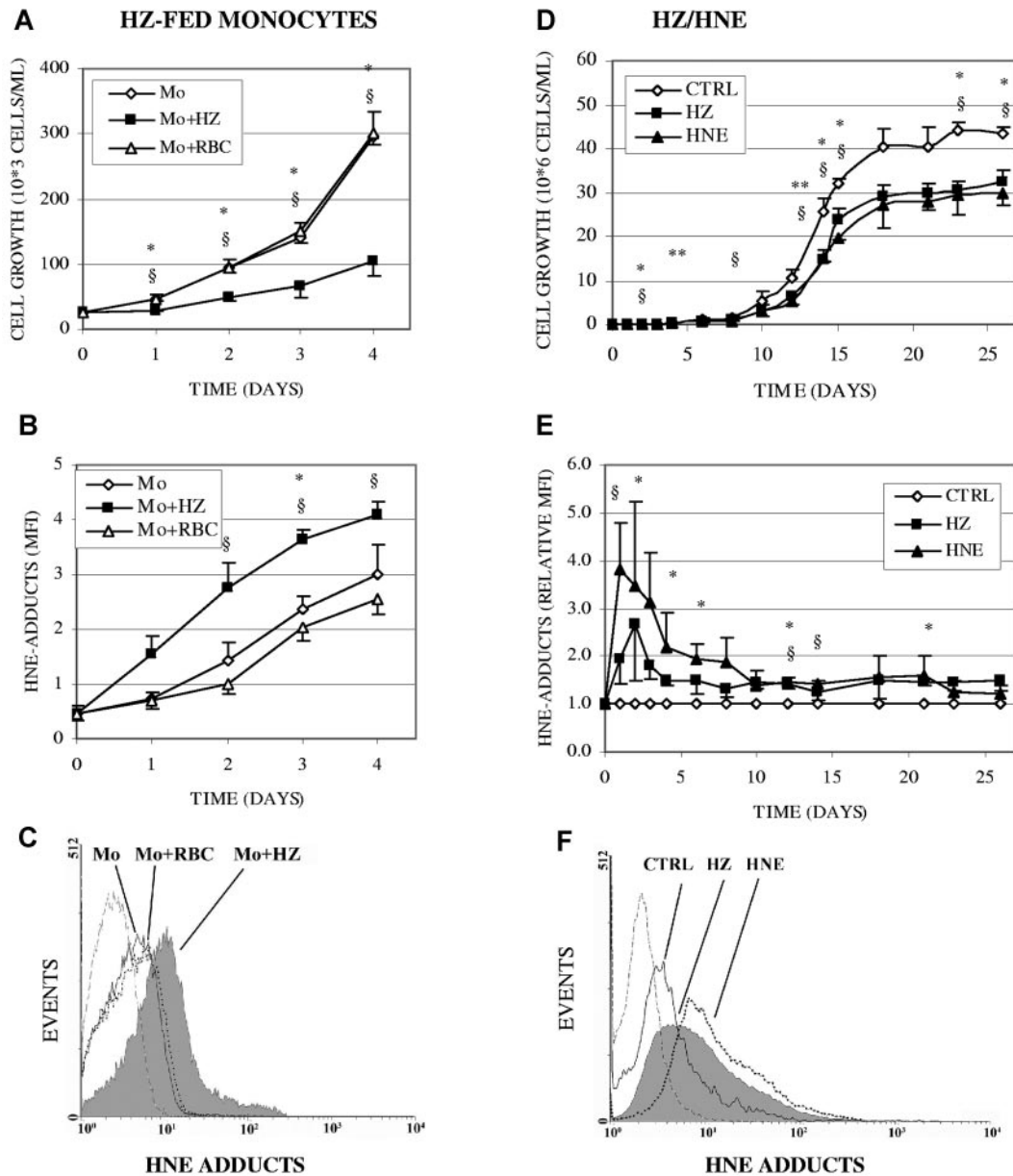


**Figure 1. Inhibition of erythroid cell growth and formation of HNE surface adducts in erythroid cells cocultivated with HZ-fed human monocytes, cocultivated with HZ, or treated with HNE.** (A-C) Erythroid cells were cocultivated with unfed (Mo), HZ-fed (Mo + HZ), or RBC-fed (Mo + RBC) monocytes in liquid culture. Adherent monocytes were unfed, fed with either HZ (25µM HZ-heme, corresponding to 12 RBCs/monocyte in terms of heme content), or 50 opsonized RBCs/monocyte for 3 hours. After removal of nonphagocytosed HZ or RBCs, erythroid cells were added to the monocytes at a cell ratio of 1:1, corresponding to a 10:1 ratio at day 4 of cocultivation. (A) Growth of erythroid cells was calculated from cell numbers counted in the expanding cultures (means ± SE of 3 independent experiments). The significance of differences ( $P < .05$ ) between erythroid cells cocultivated with HZ-fed monocytes and unfed (\*) or RBC-fed (§) cells and untreated controls and ( $P < .1$ ) between HZ-treated (\*\*) cells and controls are indicated. (B) HNE-adducts on erythroid cell surface were quantified by flow cytometry after immune staining and expressed as MFI (means ± SE of 3 independent experiments). The significance of differences ( $P < .05$ ) between HZ-treated (\*) or HNE-treated (§) cells and untreated controls are indicated. (C,F) Representative expression profiles of cell-surface HNE adducts measured by flow cytometry in erythroid cells cocultivated with HZ-fed (solid line filled space), RBC-fed (dotted line unfilled space) monocytes (C), HZ (solid line filled space), or treated with HNE (7µM; dotted line unfilled space) (F) for 1 day, and in control erythroid cells (solid line unfilled space). Background is plotted as dashed line.

As shown in Figure 3, developing control erythroid cells progressively decreased their overall ability to form colonies. Substantial growth reduction of the younger BFU-E by 65% and 90% occurred already at day 4 and day 8, respectively. The initially small population of CFU-E rose by 400% until day 4, while the cultures maintained the colony-forming capability until day 8, indicating the progress in erythroid cell differentiation in the liquid culture. Finally, on day 14 the colony-forming capacity dropped down to

zero for BFU-E and to nearly zero for CFU-E due to the disappearance of these progenitors. Cocultivation of erythroid cells with HZ or treatment with HNE inhibited the formation of both erythroid colonies by approximately 50% from the very beginning until the disappearance of BFU-E and CFU-E on day 14 (Table 1 and Figure 3). Of note, a small and fast-decreasing portion of cells developed to CFU-GM. Growth of this colony was also inhibited by HZ and HNE.

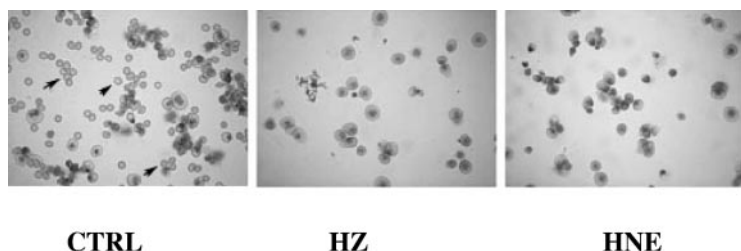


**Figure 2. Inhibition of differentiation and growth of erythroid cells cocultivated with HZ or treated with HNE.** The May-Grünwald/Giemsa stains of cytopins of cells cultivated for 21 days show numerous fully mature RBCs (arrows) in the untreated control (CTRL) cultures, and negligible numbers of fully mature RBCs in presence of HZ (25  $\mu$ M HZ-heme) or HNE (7  $\mu$ M). Differences in staining and cell size between controls and HZ/HNE-treated cells indicate the delayed differentiation caused by treatments. Optical microscope photographs (Leica DM LB, 40 $\times$ ; acquisition software: Leica DFC Twain, version 6.5.0; camera: Leica DFC 320).

### Inhibition of expression of differentiation markers hemoglobin and glycophorin A in erythroid cells cocultivated with HZ or treated with HNE

Figure 4 shows that increase in expression of hemoglobin (Figure 4A) and glycophorin A (Figure 4C,E) was lower by 30% and 50%, respectively, while decrease in expression of CD34 was slower in HZ/HNE-treated cells (Figure 4B,F) and in cells cocultivated with HZ-laden monocytes (Figure 4D). Above data together with the histologic evidence of delayed erythropoiesis (Figure 2) indicate that the loss of colony-forming capacity shown in Figure 3 and Table 1 may result from impaired growth rather than accelerated differentiation.

### Inhibition of cell cycle, enhancement of p53 and p21 protein expression, and inhibition of cyclin A and D2 expression in erythroid cells cocultivated with HZ or treated with HNE

A variety of damaging agents and oxidative stress may elicit cell-cycle inhibition or apoptosis in response to mild or severe damage, respectively.<sup>27</sup> Literature data indicate that HNE blocks the cell cycle in  $G_0/G_1$ , the gap phase that allows cells to repair alterations before progressing into replication in the S-phase, increasing the proportion of  $G_0/G_1$  cells.<sup>16</sup> We first examined the distribution of early erythroid cells treated with HZ/HNE in the different cell-cycle phases. As shown in Figure 5, incubation of erythroid cells with HZ or HNE during 3 days reduced the proportion of cells in the  $G_2/M$  phase by 61% and 72%, respectively, while the percentage of cells in  $G_0/G_1$  was correspondingly increased. This corresponds to a constant shift of 10% of the whole cell population from the dividing into the resting  $G_0/G_1$  cohort. This shift is high enough to explain the proliferation deficit in HZ/HNE-treated cells. Two observations, however, make the additional impairment of S- and  $G_2$ -phase likely. First, the size of the S-phase cohort (Figure 5B) was less diminished as expected from the decreased influx from the  $G_1$  phase with the exception of

HNE-treated cells on day 1; second, cyclin B, which promotes the entrance into mitosis, was decreased. Parallel studies performed with K562 cells indicated that their treatment with HZ/HNE led to a similar slowdown of the cell cycle (supplemental Figure 3).

In search for a mechanism explaining the HZ/HNE-mediated cell-cycle inhibition, we analyzed the p53-p21 system, one major pathway that controls the expression of the cyclins needed for cell-cycle progress.<sup>17,18</sup> Western blot data demonstrate a progressive increase of p53 in the HZ/HNE-treated cells with 4- to 5-fold increase already at day 1 (Figure 6A). Consequently, the expression of the kinase inhibitor p21 was increased approximately 5- and 12-fold in HNE- and HZ-treated cells, respectively (Figure 6B). In the K562 cell line, treatment with HZ/HNE increased p21 expression approximately 2-fold and the share of low-phosphorylated retinoblastoma protein pRb by 40% (supplemental Figure 4A-B). Low-phosphorylated pRb inhibits the transcription factor E2F, which controls cyclin expression. This data are consistent with the reduced expression of cyclin A, B, and D2 (Figure 6C-D and supplemental Figure 4C-E) and the inhibition of the cyclin-dependent kinase 2 (Cdk 2) as concluded from the low phosphorylation degree of pRb (supplemental Figure 4B) and in accordance with cell-cycle slowdown in  $G_1$ . Due to the reduced expression of cyclin A and B (Figure 6C and supplemental Figure 4C,E), an additional cell-cycle retardation in the S- and the  $G_2$ -phase is likely.

### Inhibition by HZ and HNE of TfR, SCFR, EPOR, IL-3R, and GATA-1 expression

Induction of p53 has been recently shown to modulate expression of TfR1, which plays a prominent role in cellular iron uptake and regulation of ferritin.<sup>28,29</sup> Indeed, we show here that the protein expression of TfR1 was decreased after HZ/HNE-treatment (Figure 7A-C,F). HZ provoked an early and irreversible loss in mean TfR1 expression on the cell surface along the whole period of ex vivo erythropoiesis, amounting to 80% expression of controls on day

**Figure 3. Inhibition of BFU-E and CFU-E colony formation in erythroid cells cocultivated with HZ or treated with HNE.** Primary erythroid cell cultures were cocultivated with HZ (25  $\mu$ M HZ-heme), treated with HNE (7  $\mu$ M), or kept as untreated controls (CTRL). At indicated times cells were taken from the liquid culture and  $10^3$  cells were seeded in semisolid medium to assess their BFU-E, CFU-E, and CFU-GM colony-forming ability. One representative experiment of 5 is shown.

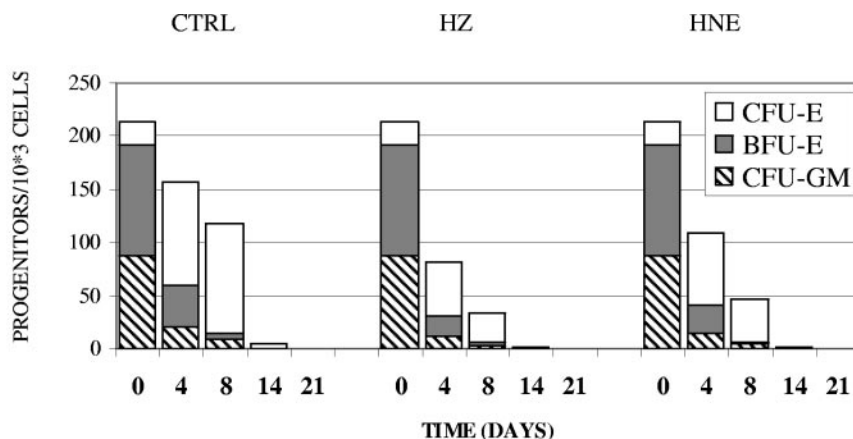


**Table 1. Inhibition of BFU-E and CFU-E colony formation by HZ and HNE**

	CFU-E		BFU-E		CFU-GM	
	Mean (SE)	n	Mean (SE)	n	Mean (SE)	n
<b>Day 4</b>						
HZ	59.2* (15.4)	5	54.6* (14.3)	5	76.2 (10.5)	5
HNE	51.3* (12.0)	5	68.2* (10.4)	5	84.6 (8.1)	5
<b>Day 8</b>						
HZ	51.4* (8.1)	4	51.8* (18.7)	4	43.2* (5.8)	4
HNE	37.3* (12.8)	4	53.7* (18.1)	4	61.8* (11.4)	4
<b>Day 14</b>						
HZ	35.8* (6.3)	5	no colonies	5	no colonies	5
HNE	45.9* (28.6)	5	no colonies	5	no colonies	5

Growth inhibition in cultures supplemented with HZ and HNE is shown as percentage of control cell growth. Erythroid cells were cocultivated with HZ (25µM HZ-heme) or treated with HNE (7µM final concentration) or kept as untreated controls. At indicated times, 10<sup>3</sup> cells were seeded in semisolid medium to assess their colony-forming ability. \*Significant difference (*P* < .05) between HZ-treated or HNE-treated cells and controls.

1 and 75% at day 6, maintaining this low value until day 14 (Figure 7B). The share of TfR1 highly positive cells declined similarly during the study period (Figure 7A). The reduction of TfR1 was not limited to the cell surface, but was also found in the protein extract from the whole-cell lysate during the study period, as shown in one representative Western blot on day 1 of ex vivo erythropoiesis (Figure 7C). The same result was observed when erythroid cells were cocultivated with HZ-fed monocytes (Figure 7D).

The expression of crucial receptors and progression along a regular erythroid growth is dependent on GATA-1, the key transcription factor for surface receptors in erythroid cells.<sup>19</sup> Compared with control cells, GATA-1 protein expression was

decreased by 55% and 49% in erythroid cells cocultivated for 6 days with HZ or HNE, respectively (Figure 7E). Pilot studies indicate furthermore an early onset of GATA-1 repression already detectable at day 1 of cocultivation (not shown). The surface expression of SCFR, EPOR, and IL-3R was analyzed (Figure 7B,D,F). HZ and HNE treatment decreased the surface expression of SCFR by 30% and 40%, respectively, already on day 1 after start of treatments (Figure 7B), and cells did not recover until day 14. The surface expression of EPOR decreased by approximately 70% on day 1-2 after start of treatments, and remained low for further 14 days along the period of high EPOR expression in control cells (Figure 7B). As expected, the expression of EPOR decreased

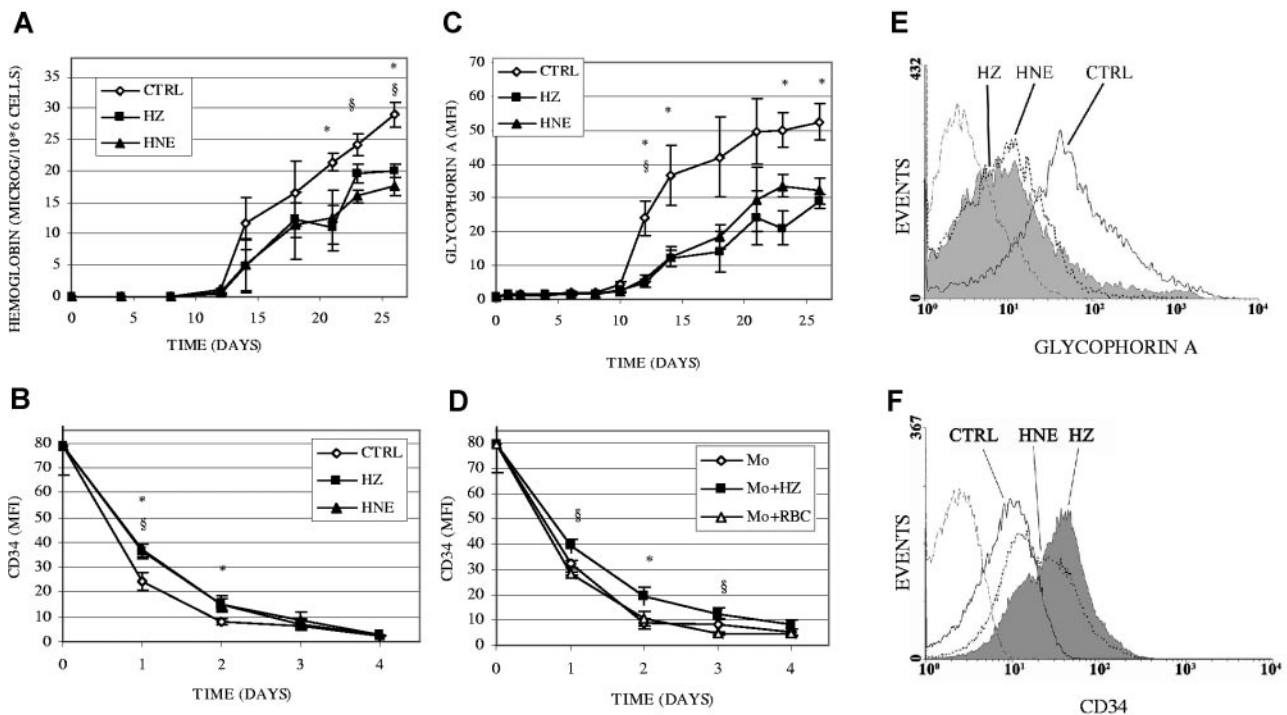


**Figure 4. Inhibition of expression of differentiation markers hemoglobin and glycoprotein A and impaired disappearance of CD34 in erythroid cells cocultivated with HZ or treated with HNE.** (A-C) Erythroid cells were cocultivated with HZ (25µM HZ-heme), treated with HNE (7µM), or kept as untreated controls (CTRL) in liquid culture. (A) Cellular hemoglobin was quantified by the Drabkin method and expressed as micrograms per 10<sup>6</sup> cells. (B) The surface expression of CD34 and (C) glypophorin A was quantified by flow cytometry after immune staining and expressed as MFI. (D) CD34 expression was monitored in erythroid cells cocultivated with unfed (Mo), HZ-fed (Mo + HZ) (25µM HZ-heme, corresponding to 12 RBCs/monocyte in terms of heme content), or RBC-fed (Mo + RBC) monocytes (50 RBCs/monocyte). Means ± SE of 3 independent experiments. The significance of differences (*P* < .05) between untreated and HZ- (\*) or HNE-treated (§) cells (A-C), or between erythroid cells cocultivated with HZ-fed monocytes and unfed (\*) or RBC-fed monocytes (§; D) are indicated. (E-F) GlypophorinA and CD34 measured by flow cytometry in erythroid cells at days 15 and 1 of cocultivation with HZ (solid line filled space) and HNE (dotted line unfilled space) and in control erythroid cells (solid line, unfilled space). Background is plotted as dashed line.

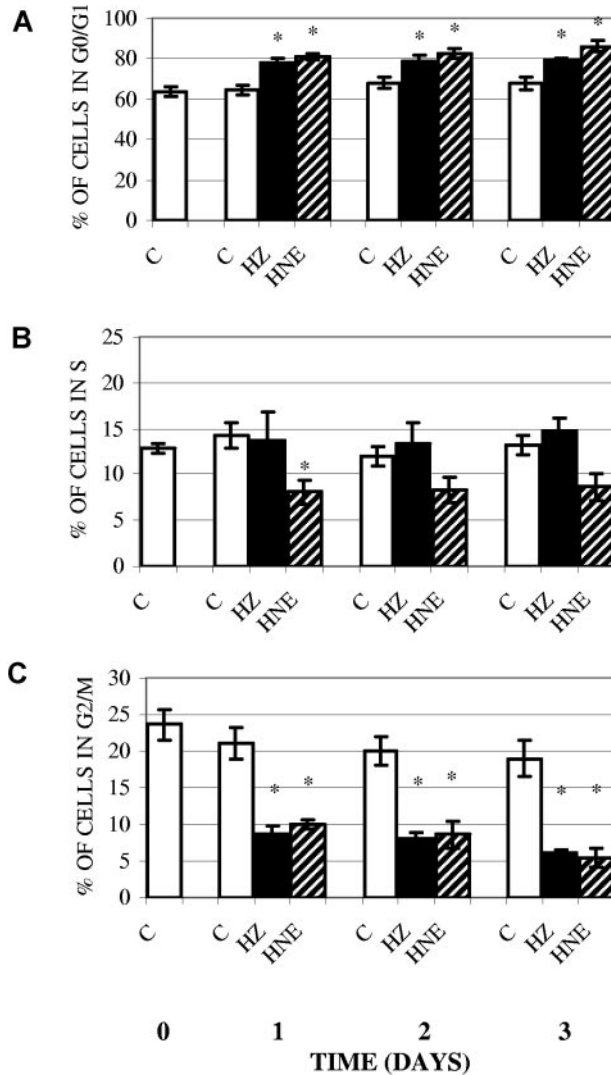


**Figure 5. Inhibition of cell cycle in erythroid cells cocultivated with HZ or treated with HNE.** Erythroid cells were cocultivated with HZ (25 μM HZ-heme), treated with HNE (7 μM), or kept as untreated controls (C) in liquid culture. For assessment of cell cycle, cells were stained with PI and analyzed for DNA content by flow cytometry. Percentage of cells in G<sub>0</sub>/G<sub>1</sub> (A), S (B), and G<sub>2</sub>/M (C) phase of cell cycle was determined. Means ± SE of 5 independent experiments. The significance of differences (\**P* < .05) between controls and HZ-treated or HNE-treated cells are indicated.

gradually to zero in higher differentiated erythroid cell controls as it did in treated cultures (data not shown). Compared with HZ effect, HNE-mediated decrease of EPOR expression was approximately 50% lower along the whole study period (Figure 7B). Similar to HZ, HNE-mediated inhibition was observed also for IL-3R expression, where 40% and 20% inhibition was detected after HZ and HNE treatment, respectively (Figure 7B). A less severe impairment of these receptors was observed when erythroid cells were coincubated with HZ-fed monocytes (Figure 7D).

### Discussion

This in vitro study confirms the inhibitory role of malaria pigment HZ on erythropoiesis,<sup>8,15</sup> describes the HZ-mediated slowdown of cell cycle and inhibition of crucial receptors, identifies HNE, a HZ-generated product, as one responsible molecule, and suggests a

mechanistic interpretation for above effects. The study was first performed with HZ-laden monocytes cocultivated with erythroid cells, in an attempt to simulate the erythroblastic island in the BM of malaria patients, where erythroid precursors grow in close contact to a central macrophage frequently laden with HZ. Having shown that HZ-laden monocytes shed HNE that diffuses to the adjacent erythroid cells and inhibits their growth and differentiation, most subsequent studies were performed with human erythroid and K562 cells directly cocultivated with HZ or supplemented with low-micromolar HNE (7 μM) to avoid confounding factors produced by HZ-laden monocytes. The HNE concentration used here was not cytotoxic but recapitulated effects observed in the BM of malaria patients.<sup>6-8</sup> As discussed below, study models are simplifications of the in vivo situation, where other molecules (such as tumor necrosis factor [TNF] and macrophage inhibitory factor, MIF) produced by HZ-laden phagocytes and by other BM cells may play an additional inhibitory role.

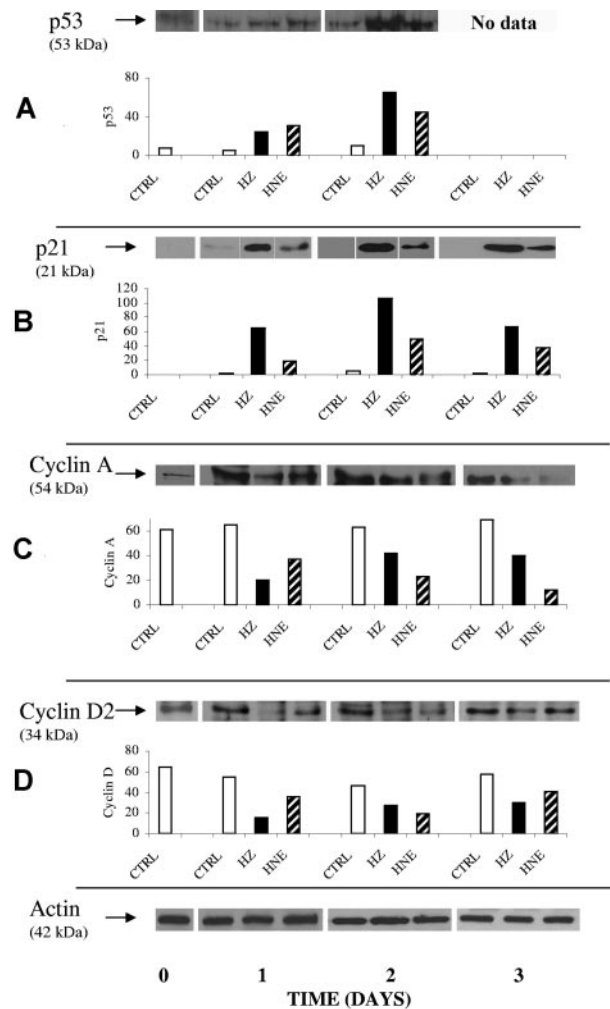


**Figure 6. Enhancement of p53 and p21 protein expression and inhibition of expression of cyclin A and D2 in erythroid cells cocultivated with HZ or treated with HNE.** Erythroid cells were cocultivated with HZ (25 μM HZ-heme) or treated with HNE (7 μM) or kept as untreated controls (CTRL) in liquid culture. At indicated times cells were harvested, and 20 μg of lysate protein were analyzed for protein expression of p53 (A), p21 (B), cyclin A (C), and cyclin D2 (D). Proteins were separated by 1-dimensional (1D) SDS-PAGE and Western blotted. Transferred proteins were probed with specific primary antibodies and detected by binding of appropriate secondary antibodies. ECL-evidenced proteins of one representative experiment of 3. The corresponding densitometric values for each protein (arbitrary units) and the actin loading control are presented.

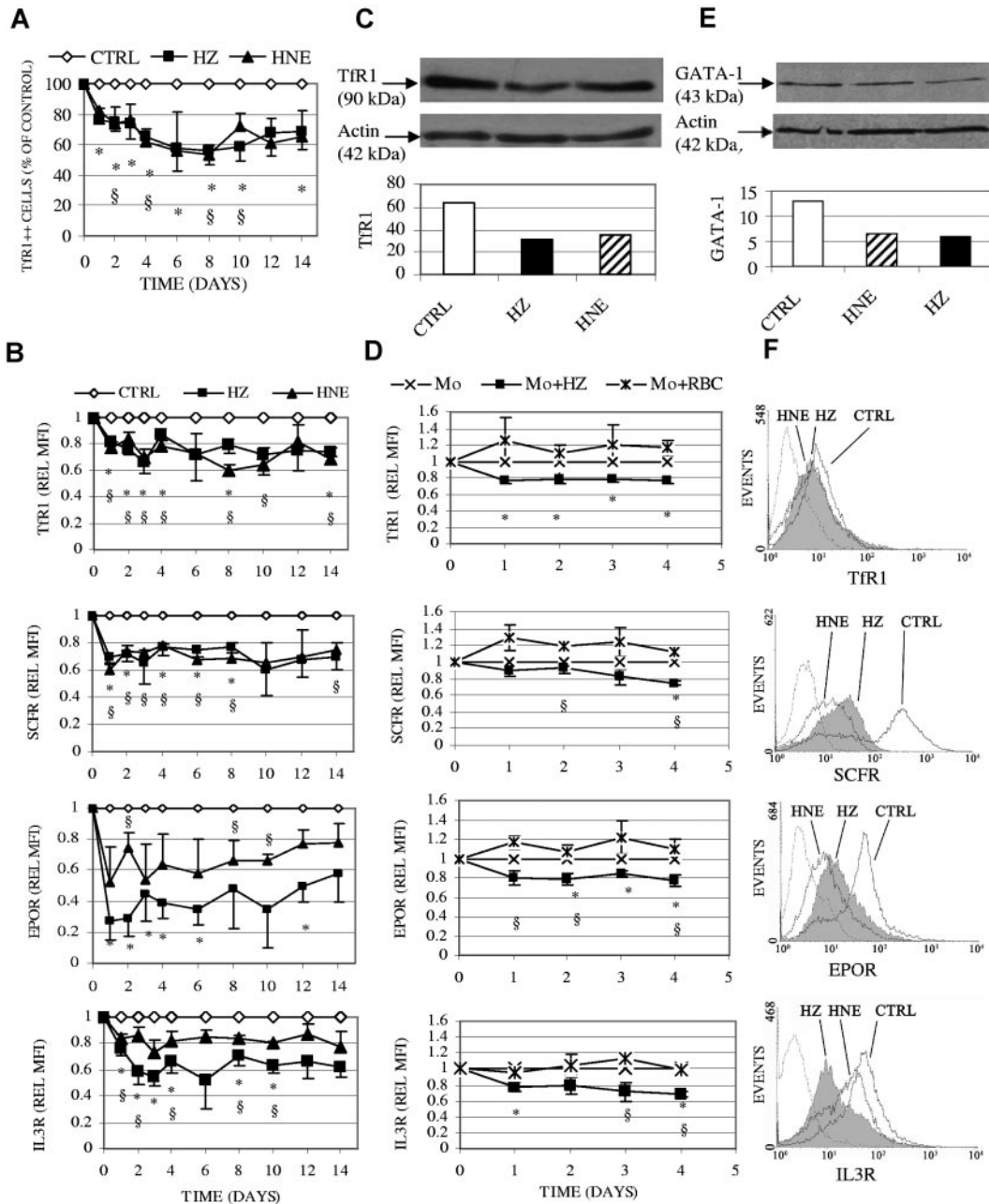


**Figure 7. Inhibition of surface expression of Tfr1, SCFR, EPOR, IL-3R, and of total protein of Tfr1 and GATA-1 in erythroid cells cocultivated with HZ or treated with HNE.** Erythroid cells were cocultivated with HZ (25 $\mu$ M HZ-heme), treated with HNE (7 $\mu$ M), or kept as untreated controls (CTRL) in liquid culture. (D) Erythroid cells were cocultivated with unfed (Mo), HZ-fed (Mo + HZ), or RBC-fed (Mo + RBC) monocytes in liquid culture. (A-B,D) The surface expression of antigens was quantified by flow cytometry after immune staining and expressed in panel A as the percentage of Tfr1 highly positive treated cells referred to highly positive control cells and in panels B and D as relative MFI (REL MFI). Relative MFI is the ratio of the MFIs of treated to untreated cells. Means  $\pm$  SE of 3 or more independent experiments. The significances of differences ( $P < .05$ ) between controls and HZ-treated (\*) or HNE-treated (§) cells (A-B), or between erythroid cells cocultivated with HZ-fed monocytes and unfed (\*) or RBC-fed (§) monocytes are indicated (D). (C-E) Total protein expression of Tfr1 (C) and GATA-1 (E) was analyzed in 15  $\mu$ g and 30  $\mu$ g lysate protein from cells harvested on days 1 and 6 after addition of HZ/HNE. Proteins were separated by 1-dimensional SDS-PAGE and Western blotted. Transferred proteins were probed with specific primary antibodies and detected by binding of appropriate secondary antibodies. Tfr1 and GATA-1 evidenced by ECL and the densitometric analysis are shown. One representative experiment of 3 is shown. Actin is included as loading control. (F) Representative expression profiles of cell surface Tfr1, SCFR, EPOR, and IL-3R measured by flow cytometry in erythroid cells after 1 day coincubation with HZ (solid line filled space) and HNE (dotted line unfilled space); control erythroid cells plotted as solid line/unfilled space and background as dashed line/unfilled space.

A first major result of this study was the observation that all 3 experimental models—cocultivation with HZ-laden monocytes; cocultivation with isolated HZ; and direct HNE supplementation—displayed inhibition of erythroid cell growth accompanied by formation of HNE adducts. Surprisingly, cell growth inhibition elicited by the HZ/HNE treatments was not the result of apoptosis,

but appeared to be due to cell-cycle inhibition. The increased percentage of G<sub>0</sub>/G<sub>1</sub> cells, the parallel decrease of G<sub>2</sub>/M cells and the decreased expression of cyclin D2 indicate that HZ/HNE treatment inhibited the cycle at checkpoint G<sub>1</sub>, governed by the D- and E-type cyclins, and cyclin-dependent kinases cdk2, cdk4, and cdk6. The additional decrease of A- and B-cyclin suggests that



the S- and G<sub>2</sub>-phase were also retarded contributing to the overall slowdown of the cycle. Inhibition of DNA polymerase- $\alpha$  by HNE may also contribute to cell-cycle delay.<sup>14</sup> Interestingly, reports have shown changes in the cell-cycle distribution in erythroblasts and ineffective erythropoiesis in BM aspirates of Gambian children<sup>10</sup> and non- and semi-immune adults<sup>4</sup> suffering from malaria anemia.

In search of mechanisms connecting HNE with the slowdown of cell cycle, we focused on the transcription factor p53, an important regulator of the cell cycle, involved in both G<sub>1</sub> and G<sub>2</sub> checkpoints.<sup>17</sup> DNA damage, redox stress, and other stress-related signals stabilize p53 and increase its protein level through posttranslational modifications.<sup>30</sup> Low-extent damage increases p53 accumulation in the nucleus up-regulating prosurvival pathways and DNA repair genes, finally slowing down cell cycle or promoting cell-cycle arrest. Whether the cell undergoes cell-cycle arrest or apoptosis depends on the extent of p53 increase, the presence of extracellular survival factors, and the availability of additional transcription factors.<sup>30,31</sup> In this study, HZ/HNE-treated cells enhanced the protein expression of p53 and cdk-inhibitor p21, inducing a shift in the phosphorylation state of the retinoblastoma protein (Rb) in favor of the low-phosphorylated form (pRb).<sup>18</sup> pRb inactivates the transcription factor E2F, which controls cyclin A, cyclin D, and cdk2, resulting in delay of the G<sub>1</sub> and S phase and slowdown of cell cycle.<sup>18</sup> HNE was shown to increase expression of p53 and p21 in a variety of cells and inhibited cell cycle at low micromolar concentrations, while higher concentrations resulted in apoptosis.<sup>14,16,32</sup> p53 is enhanced by covalent modifications (phosphorylation, acetylation, and others) that inhibit its degradation.<sup>30</sup> HNE may add to those covalent p53 modifiers.<sup>33,34</sup> In addition, HNE was shown to bind to guanine residues in DNA possibly generating a DNA-damage signal that may phosphorylate and stabilize p53.<sup>35</sup> As a first partial conclusion, above data may provide a mechanistic explanation on how HZ and HNE generated in the BM may slow down erythropoiesis and establish a causal link with malaria anemia.

A second major result was the HZ/HNE-mediated inhibition of the protein expression of TfR1, EPOR, SCFR, and IL-3R. We suggest a mechanistic connection between receptors inhibition and the modified expression of p53 and p21. Firstly, in analogy with other studies,<sup>28,29</sup> up-regulation of p53 and p21 may decrease the TfR1 levels by down-regulating iron regulatory protein 2, which stabilizes the TfR1-mRNA. Iron regulatory protein 2 may be directly hindered by HNE-adduction to C512 and C516 cysteine residues crucial for RNA binding and targets of oxidative modifications.<sup>36</sup> Repression of TfR1 may restrict availability of intracellular iron and limit cell-cycle progression.<sup>37</sup> Iron is critical for cell growth and proliferation in as much as it is required for the activity of ribonucleotide reductase, the essential enzyme for de novo DNA synthesis, and is an essential cofactor of the G<sub>1</sub> and S phase cyclins.<sup>38</sup> Secondly, increased p53 was shown to inhibit the activation of GATA-1 responsive genes.<sup>39</sup> GATA-1 is a multifunctional zinc-finger DNA-binding protein considered to be the master transcription factor for erythroid differentiation and expression of erythroid gene products, such as EPOR, SCFR, IL-3R, and GATA-1 itself.<sup>19,40,41</sup> In this study we have indeed shown that HZ/HNE treatment mediated the down-regulation of GATA-1, possibly occurring via p53, which by itself may explain the low expression levels of EPOR, SCFR, and IL-3R and the impaired differentiation and growth observed here. The direct binding of the pRb/E2F-complex to GATA-1 could further inhibit maturation and proliferation of erythroid precursors.<sup>42</sup> Putative covalent modifications of redox-sensitive cysteine and easily accessible

lysine residues by HNE in the DNA-binding region of GATA-1 might be critical for DNA binding and transcriptional activity and were proposed to have a regulatory function in erythroid differentiation.<sup>43</sup>

Our data agree with the HZ-dependent delay during the initial phase of erythroid differentiation previously reported.<sup>8,15</sup> However, in contrast to present data, HZ-dependent apoptosis was noted in approximately 10% of basophilic erythroblasts.<sup>44</sup> Apoptosis observed in these cells may be due, firstly, to the presence of contaminating monocytes and T cells that may produce cytotoxic factors during erythroblast expansion and differentiation; secondly, to the absence of antiapoptotic IL-3 in the medium; and lastly, to HZ addition to cells at a late differentiation stage.

We do not exclude that in vivo HZ-laden BM phagocytes may produce inhibitory cytokines such as TNF or MIF.<sup>45,46</sup> However, in CD34<sup>+</sup> progenitor expansion experiments, TNF levels lower than 3 ng/mL did not inhibit erythropoiesis.<sup>8</sup> In vivo data obtained from patients with SMA show TNF plasma levels not higher than 100 pg/mL, clearly insufficient to inhibit erythropoiesis.<sup>47,48</sup> MIF production by murine macrophage-fed artificial HZ ( $\beta$ -hematin) was enhanced,<sup>46</sup> but MIF plasma levels in malaria patients negatively correlated with malaria severity.<sup>49</sup> Taken together, those data do not support a significant inhibitory role at least of those cytokines in vivo.

In conclusion, previous studies have shown direct inhibition of erythropoiesis by HZ in vitro, and a correlation between HZ levels in circulating monocytes and altered erythropoiesis and anemia in vivo.<sup>1,8,15,50</sup> Present data indicate that HNE, a very potent terminal aldehyde of lipid peroxidation generated by the catalytic activity of HZ-iron,<sup>11-13</sup> might be a specific culprit of erythropoiesis inhibition. Two major effects described here were elicited by coincubating HZ-fed human monocytes with developing erythroid cells and recapitulated by coincubation with native HZ or treatment with low micromolar, noncytotoxic concentrations of HNE. Firstly, all treatments induced growth inhibition of developing erythroid cells interfering with cell cycle without inducing apoptosis. Two critical proteins in cell-cycle regulation, p53 and p21, were increased and the central regulator of G<sub>1</sub>- to S-phase transition, the retinoblastoma protein, was consequently hypophosphorylated. The resultant decrease of cyclins A and D2 expression retarded cell cycle progression without apoptosis. Secondly, treatments inhibited the expression of the transcription factor GATA-1 and of the receptors TfR1, SCFR, IL-3R, and EPOR, crucial for erythropoietic differentiation. The reduced receptor expression together with the impaired cell cycle decreased the total production of erythroid cells as well as the yield of differentiated erythroid cells expressing glycophorin A and hemoglobin at the end of growth. Taken together, present data may provide a mechanistic explanation for the inhibition of erythropoiesis in malaria anemia and offer an experimental scaffold for in vivo testing.

## Acknowledgments

This work was supported by Regione Piemonte, Progetto Ricerca Scientifica Applicata, and Progetti Ricerca Sanitaria Finalizzata (to E.S., P.A., W.P., and T.M.), Associazione Italiana Ricerca sul Cancro (AIRC), Milano (to W.P.) and Compagnia di San Paolo, Italian Malaria Network Project (to P.A.).

## Authorship

Contribution: O.A.S., L.C., T.M., G.M., V.B., and E.S. conducted experiments; O.A.S., W.P., P.A., and E.S. designed experiments and interpreted results; and O.A.S., P.A., W.P., and E.S. wrote the paper.

Conflict-of-interest disclosure: The authors declare no competing financial interests.

Correspondence: Evelin Schwarzer, Dipartimento di Genetica, Biologia e Biochimica, Università di Torino, Via Santena 5 bis, 10126 Torino, Italy; e-mail: evelin.schwarzer@unito.it.

## References

- Casals-Pascual C, Roberts DJ. Severe malarial anaemia. *Curr Mol Med*. 2006;6(2):155-168.
- Chang KH, Tam M, Stevenson MM. Inappropriately low reticulocytosis in severe malarial anemia correlates with suppression in the development of late erythroid precursors. *Blood*. 2004;103(10):3727-3735.
- Burgmann H, Looareesuwan S, Kapiotis S, et al. Serum levels of erythropoietin in acute Plasmodium falciparum malaria. *Am J Trop Med Hyg*. 1996;54(3):280-283.
- Dörmer P, Dietrich M, Kern P, Horstmann RD. Ineffective erythropoiesis in acute human P. falciparum malaria. *Blut*. 1983;46(5):279-288.
- Knüttgen HJ. Das Verhalten der Makrophagen und die Phagozytose von Parasiten im Knochenmark bei Malaria tropica. *Z Tropenmed Parasit*. 1961;12:161-171.
- Phillips RE, Looareesuwan S, Warrell DA, et al. The importance of anaemia in cerebral and uncomplicated falciparum malaria: role of complications, dyserythropoiesis and iron sequestration. *Q J Med*. 1986;58(227):305-323.
- Wickramasinghe SN, Abdalla SH. Blood and bone marrow changes in malaria. *Baillieres Best Pract Res Clin Haematol*. 2000;13(2):277-299.
- Casals-Pascual C, Kai O, Cheung JO, et al. Suppression of erythropoiesis in malarial anemia is associated with hemozoin in vitro and in vivo. *Blood*. 2006;108(8):2569-2577.
- Chasis JA, Mohandas N. Erythroblastic islands: niches for erythropoiesis. *Blood*. 2008;112(3):470-478.
- Wickramasinghe SN, Abdalla S, Weatherall DJ. Cell cycle distribution of erythroblasts in P. falciparum malaria. *Scand J Haematol*. 1982;29(1):83-88.
- Schwarzer E, Kühn H, Valente E, Arese P. Malaria-parasitized erythrocytes and hemozoin nonenzymatically generate large amounts of hydroxy fatty acids that inhibit monocyte functions. *Blood*. 2003;101(2):722-728.
- Schwarzer E, Müller O, Arese P, Siems WG, Grune T. Increased levels of 4-hydroxynonenal in human monocytes fed with malarial pigment hemozoin. A possible clue for hemozoin toxicity. *FEBS Lett*. 1996;388(2-3):119-122.
- Skorokhod O, Schwarzer E, Grune T, Arese P. Role of 4-hydroxynonenal in the hemozoin-mediated inhibition of differentiation of human monocytes to dendritic cells induced by GM-CSF/IL-4. *Biofactors*. 2005;24(1-4):283-289.
- Poli G, Schaur RJ, Siems WG, Leonarduzzi G. 4-Hydroxynonenal: a membrane lipid oxidation product of medicinal interest. *Med Res Rev*. 2008;28(4):569-631.
- Giribaldi G, Ulliers D, Schwarzer E, Roberts I, Piacibello W, Arese P. Hemozoin- and 4-hydroxynonenal-mediated inhibition of erythropoiesis. Possible role in malarial dyserythropoiesis and anemia. *Haematologica*. 2004;89(4):492-493.
- Barrera G, Pizzimenti S, Dianzani MU. 4-Hydroxynonenal and regulation of cell cycle: effects on the pRb/E2F pathway. *Free Radic Biol Med*. 2004;37(5):597-606.
- Vousden KH, Prives C. Blinded by the light: the growing complexity of p53. *Cell*. 2009;137(3):413-431.
- Abbas T, Dutta A. p21 in cancer: intricate networks and multiple activities. *Nat Rev Cancer*. 2009;9(6):400-414.
- Welch JJ, Watts JA, Vakoc CR, et al. Global regulation of erythroid gene expression by transcription factor GATA1. *Blood*. 2004;104(3):3136-3147.
- Giarratana MC, Kobari L, Lapillonne H, et al. Ex vivo generation of fully mature human red blood cells from hematopoietic stem cells. *Nat Biotechnol*. 2005;23(1):69-74.
- Piacibello W, Sanavio F, Garetto L, et al. Extensive amplification and self-renewal of human primitive hematopoietic stem cells from cord blood. *Blood*. 1997;89(8):2644-2653.
- Piacibello W, Sanavio F, Bresso P, et al. Stem cell factor improvement of proliferation and maintenance of hemopoietic progenitors in myelodysplastic syndromes. *Leukemia*. 1994;8(2):250-257.
- Andersson LC, Jokinen M, Gahmberg CG. Induction of erythroid differentiation in the human leukaemia cell line K562. *Nature*. 1979;278(5702):364-365.
- Skorokhod OA, Alessio M, Mordmueller B, Arese P, Schwarzer E. Hemozoin (malaria pigment) inhibits differentiation and maturation of human monocyte-derived dendritic cells: a peroxisome proliferator-activated receptor-gamma mediated effect. *J Immunol*. 2004;173(6):4066-4074.
- Spector DL, Goldman RD, Leinwand LA, eds. *Cells: A Laboratory Manual*. Cold Spring Harbor, NY: CSH Laboratory Press; 1998.
- Darzynkiewicz Z, Juan G, Bedner E. Determining cell cycle stages by flow cytometry. *Curr Protoc Cell Biol*. 2001;Chapter 8:Unit 8.4.
- Ghaffari S. Oxidative stress in the regulation of normal and neoplastic hematopoiesis. *Antioxid Redox Signal*. 2008;10(11):1923-1940.
- Zhang F, Wang W, Tsuji Y, Torti SV, Torti FM. Post-transcriptional modulation of iron homeostasis during p53-dependent growth arrest. *J Biol Chem*. 2008;283(49):33911-33918.
- Yu Y, Kovacevic Z, Richardson DR. Tuning cell cycle regulation with an iron key. *Cell Cycle*. 2007;6(16):1982-1994.
- Brooks CL, Gu W. Ubiquitination, phosphorylation and acetylation: the molecular basis for p53 regulation. *Curr Opin Cell Biol*. 2003;15(2):164-171.
- Horvath MM, Wang X, Resnick MA, Bell DA. Divergent evolution of human p53 binding sites: cell cycle versus apoptosis. *PLoS Genet*. 2007;3(7):e127.
- Laurora S, Tamagno E, Briatore F, et al. 4-Hydroxynonenal modulation of p53 family gene expression in the SK-N-BE neuroblastoma cell line. *Free Radic Biol Med*. 2005;38(2):215-225.
- Cenini G, Sultana R, Memo M, Butterfield DA. Effects of oxidative and nitrosative stress in brain on p53 proapoptotic protein in amnesic mild cognitive impairment and Alzheimer disease. *Free Radic Biol Med*. 2008;45(1):81-85.
- Shiraishi K, Naito K. Effects of 4-hydroxy-2-nonenal, a marker of oxidative stress, on spermatogenesis and expression of p53 protein in male infertility. *J Urol*. 2007;178(3 Pt 1):1012-1017.
- Chung FL, Nath RG, Ocando J, Nishikawa A, Zhang L. Deoxyguanosine adducts of t-4-hydroxy-2-nonenal are endogenous DNA lesions in rodents and humans: detection and potential sources. *Cancer Res*. 2000;60(6):1507-1511.
- Zumbrennen KB, Wallander ML, Romney SJ, Leibhold EA. Cysteine oxidation regulates the RNA-binding activity of iron regulatory protein 2. *Mol Cell Biol*. 2009;29(8):2219-2229.
- Levy JE, Jin O, Fujiwara Y, Kuo F, Andrews NC. Transferrin receptor is necessary for development of erythrocytes and the nervous system. *Nat Genet*. 1999;21(4):396-399.
- Kulp KS, Green SL, Vulliet PR. Iron deprivation inhibits cyclin-dependent kinase activity and decreases cyclin D/CDK4 protein levels in asynchronous MDA-MB-453 human breast cancer cells. *Exp Cell Res*. 1996;229(1):60-68.
- Trainor CD, Mas C, Archambault P, Di Lello P, Omichinski JG. GATA-1 associates and inhibits p53. *Blood*. 2009;114(1):165-173.
- Rylski M, Welch JJ, Chen YY, et al. GATA-1-mediated proliferation arrest during erythroid maturation. *Mol Cell Biol*. 2003;23(14):5031-5042.
- Miyajima I, Levitt L, Hara T, et al. The murine interleukin-3 receptor alpha subunit gene: chromosomal localization, genomic structure, and promoter function. *Blood*. 1995;85(5):1246-1253.
- Kadri Z, Shimizu R, Ohneda O, et al. Direct binding of pRb/E2F-2 to GATA-1 regulates maturation and terminal cell division during erythropoiesis. *PLoS Biol*. 2009;7(6):e1000123.
- Wu X, Bishopric NH, Discher DJ, Murphy BJ, Webster KA. Physical and functional sensitivity of zinc finger transcription factors to redox change. *Mol Cell Biol*. 1996;16(3):1035-1046.
- Lamikanra AA, Theron M, Kooij TW, Roberts DJ. Hemozoin (malarial pigment) directly promotes apoptosis of erythroid precursors. *PLoS ONE*. 2009;4(12):e8446.
- Clark IA, Budd AC, Alleva LM, Cowden WB. Human malarial disease: a consequence of inflammatory cytokine release. *Malar J*. 2006;5:85.
- Martiney JA, Sherry B, Metz CN, et al. Macrophage migration inhibitory factor release by macrophages after ingestion of Plasmodium chabaudi-infected erythrocytes: possible role in the pathogenesis of malarial anemia. *Infect Immun*. 2000;68(4):2259-2267.
- McGuire W, Knight JC, Hill AV, Allsopp CE, Greenwood BM, Kwiatkowski D. Severe malarial anemia and cerebral malaria are associated with different tumor necrosis factor promoter alleles. *J Infect Dis*. 1999;179(1):287-290.
- Kurtzhals JAL, Adabayeri V, Goka BQ, et al. Low plasma concentrations of interleukin 10 in severe malarial anaemia compared with cerebral and uncomplicated malaria. *Lancet*. 1998;351(9118):1768-1772.
- Awandare GA, Ouma Y, Ouma C, et al. Role of monocyte-acquired hemozoin in suppression of macrophage migration inhibitory factor in children with severe malarial anemia. *Infect Immun*. 2007;75(1):201-210.
- Lyke KE, Diallo DA, Dicko A, et al. Association of intraleukocytic P falciparum malaria pigment with disease severity, clinical manifestations, and prognosis in severe malaria. *Am J Trop Med Hyg*. 2003;69(3):253-259.